ELSEVIER

Journal of Structural Geology 28 (2006) 253–267

JOURNAL OF STRUCTURAL GEOLOGY

www.elsevier.com/locate/jsg

Modeling dislocation creep as a near-field material transfer process during spherical pluton expansion: implications for strain rates and their preservation in pluton aureoles

Markus Albertz [a,*], Scott E. Johnson [b]

[a] *Department of Earth Sciences, University of Southern California, Los Angeles, CA 90089-0740, USA*
[b] *Department of Earth Sciences, University of Maine, Orono, ME 04469-5790, USA*

Received 1 May 2005; received in revised form 21 September 2005; accepted 1 October 2005
Available online 7 November 2005

Abstract

In this paper we model coupled spatial and temporal changes in stress and temperature to calculate dislocation creep strain rates in host rock associated with spherical magma chamber expansion with and without material removal by stoping and/or assimilation. Given a constant magma-chamber pressure of 100 MPa, we show that stress and temperatures in the host rock range from 100 to 10 MPa and 800 to 300 °C, respectively. Using a flow law for dislocation creep of wet quartzite with recently calibrated parameters, maximum dislocation creep strain rates on the order of ca. 10^{-10} s^{-1} occur only close to the pluton margin. Despite the simple geometry relative to real plutons, the models yield several thought-provoking predictions. If the outer portions of the pluton are allowed to cool, a wide thermal and structural aureole forms. Maintaining the liquidus temperature in the entire pluton allows for rapid aureole deformation, resulting in a narrow thermal and structural aureole, because the deformation outpaces heat conduction. Dislocation creep strain rates in the inner portions of aureoles are extremely sensitive to pressure changes only, potentially resulting in large transient variations in strain rate under isothermal conditions. Evidence for elevated strain rates in pluton aureoles may not be preserved in host rock aureoles if solidified pluton participates in the deformation or it may be completely removed.

Keywords: Dislocation creep; Strain rate; Pluton; Stress; Temperature; Expansion; Stoping; Assimilation

1. Introduction

Unusually large volumes of magma have been emplaced over relatively short time intervals in magmatic arcs around the world. For example, in the Sierra Nevada, California, the Sierra Crest magmatic event (ca. 98–86 Ma) resulted in more than 4000 km^2 of granitoids now exposed in map view (Bateman, 1992; Coleman and Glazner, 1997). Given that displacement of an equal amount of host rock is required to accommodate the magma, an obvious question arises: by what mechanism(s) is this host rock displaced? Buddington (1959) and Paterson et al. (1996) have suggested that the construction of large crustal magma chambers involves multiple material transfer processes (MTPs, e.g. doming, stoping, ductile deformation, translation, volume loss, assimilation). However, the contribution of any particular MTP to the overall space accommodation ultimately is controlled by which underlying grain-scale deformation mechanisms (e.g. dislocation or diffusion creep, cataclastic deformation) are active and how fast they operate at the local conditions of pressure, temperature and differential stress.

Strain rates in pluton aureoles are currently a subject of considerable interest. For example, several field and microstructural studies of individual plutons suggest that strain rates associated with displacement in aureoles lie in a range of 10^{-8}–10^{-13} s^{-1} (e.g. Karlstrom et al., 1993; John and Blundy, 1993; Miller and Paterson, 1994; Nyman et al., 1995; McCaffrey et al., 1999; Fernandez and Castro, 1999; Johnson et al., 2004). Some of these rates are several orders of magnitude higher than regional strain rates, which are

* Corresponding author. Now at: Department of Oceanography, Dalhousie University, 1355 Oxford Street, Halifax, Nova Scotia, Canada B3H 4J1. Tel.: +1 902 494 6300; fax: +1 902 494 3877.
E-mail address: markus.albertz@dal.ca (M. Albertz).

0191-8141/$ - see front matter © 2005 Elsevier Ltd. All rights reserved.
doi:10.1016/j.jsg.2005.10.002

generally considered to vary between 10^{-13} and 10^{-15} s^{-1} (e.g. Price, 1975; Pfiffner and Ramsay, 1982). However, evidence for deformation mechanisms, particularly those that can accommodate fast strain rates, can be difficult to recognize in aureoles and other geologic settings because subsequent deformation and/or thermal events can modify or completely destroy microstructures (e.g. Knipe, 1990).

The objective of this study is to numerically examine host rock strain rates associated with ductile, near-field material transfer in pluton aureoles. We employ a coupled thermo-mechanical model of spherical pluton expansion and calculate rates of dislocation creep in the surrounding aureole as a function of position and time. Although a spherical geometry deviates from natural plutons to varying degrees, we employ this simple geometry because: (1) calculation of strain rates around a growing spherical pluton as a function of temporal and spatial changes in pressure and temperature is straightforward, (2) a spherical geometry provides more conservative lateral strain rates than a vertically thin spheroid, (3) we can directly compare our results with two published kinematic models of dike-fed spherical pluton expansion (Johnson et al., 2001; Gerbi et al., 2004), and (4) mature magma chambers may approach an ellipsoidal shape (Gudmundsson, 1990).

Although ductile flow is an important material transfer process in pluton aureoles, finite strain analyses in aureoles suggest that only 30–40% of the necessary material displacement can be accommodated by ductile flow. Thus, other processes, such as stoping and/or assimilation, may play an important role. In this paper we focus on the possible role of dislocation creep as the accommodating mechanism for high strain rate ductile flow in pluton aureoles. To simulate mid- to upper-crustal conditions, we use the calibrated flow law for wet quartzite presented by Hirth et al. (2001). Transient temperature variations are simulated by a finite difference formulation for heat conduction from the growing magma chamber. We investigate the effect of coupled stress and temperature on strain rates and ultimately on the growth behavior using three end member models: (1) constant liquidus temperature in the pluton center and deformation in host rock only; (2) constant liquidus temperature in the pluton center and deformation in host rock as well as in the cooled pluton; and (3) constant liquidus temperature in the entire pluton and deformation in host rock only.

2. Material transfer during pluton emplacement

Emplacement of plutons into the crust requires that the material around growing magma chambers is displaced and accommodated someplace. The consequence of needing space for magma in the crust has long been known as the classical room problem in pluton studies. Paterson and Fowler (1993) suggested that displacement in the immediate aureole hosting a magma body does not provide the space necessary for an intrusion. The authors proposed that, besides volume loss or elastic contraction, new space can be made only by larger-scale processes, for example raising the Earth's surface, lowering the Moho, or some combination of the aforementioned. Accordingly, Paterson and Fowler (1993) proposed the usage of the terms near-field and far-field material transfer processes (MTPs) to describe displacement of material immediately in front of the magma and eventually moving this material away from the immediate aureole, respectively, for example towards the surface or back into the sites of magma generation.

Several lines of observation indicate that out-of-aureole displacement of host rock commonly involves vertical material transfer. For example, nearly ubiquitous steeply plunging stretching lineations (e.g. McNulty et al., 1996; Johnson et al., 2003; Albertz et al., 2005) and the general lack of corresponding far-field deflection of horizontal near-field bending of pre-emplacement markers (e.g. Paterson et al., 1996) in many aureoles suggest that near-field lateral shortening is accommodated by vertical flow. However, any evidence for near-field MTPs that operated in off-map sections and in particular for far-field MTPs, is typically not preserved in exposed aureoles (Fig. 1). Additionally, the rates of far-field MTPs are expected to be much lower than

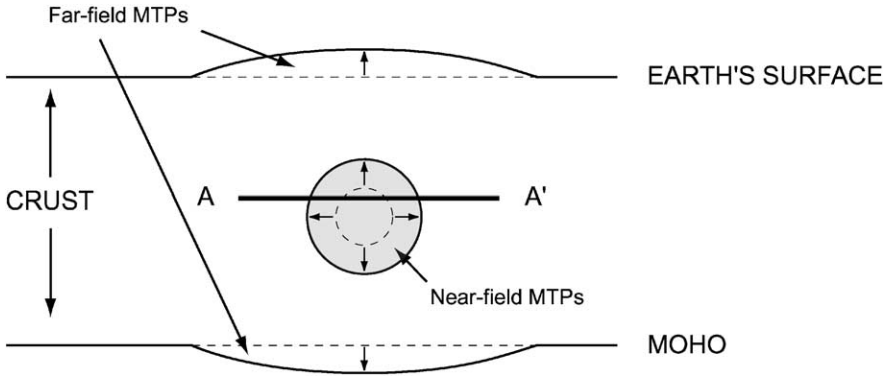

Fig. 1. Schematic illustration of near-field and far-field material transfer processes (MTPs) associated with pluton emplacement (not to scale). Shaded region depicts growing pluton. Material displaced by near-field MTPs in the immediate aureole is transported out of the aureole towards the Earth's surface and/or back to the source region via far-field MTPs. Line A–A′ depicts typically preserved section of a pluton in the field.

those of near-field MTPs, because the wall rock volume affected by far-field MTPs increases by r^3 (where r is the radial distance from the pluton center; Paterson and Fowler, 1993). Hence, strains indicative of far-field MTPs are likely to be too small to be recognized.

Gerbi et al.'s (2004) kinematic modeling successfully provided insight into strain rate variations associated with spherical expansion without explicitly incorporating far-field MTPs, such as surface uplift and return flow to the source region. Because we are similarly interested in evaluating order-of-magnitude changes of strain rates in a spherical shell surrounding a growing pluton, we take the same approach and neglect far-field MTPs and the associated vertical material transfer. In this study, we focus on ductile flow as a representative end-member, near-field MTP.

Ductile flow has been recognized in many pluton aureoles around the world and hence finite strains obtained from field-based studies can be directly compared with theoretical models of pluton growth. We note that despite the common recognition of ductile flow in aureoles, however, it may not be the only near-field MTP to accommodate material displacement associated with chamber growth of natural plutons. Marker deflections and measurements of ductile strain in many natural aureoles indicate that most of those evaluated recorded enough bulk shortening to account for ca. 30–40% of the material displacement necessary for magma emplacement (Paterson and Vernon, 1995). The remaining 60–70% of the material displacement is thought to be accommodated by other processes. For example, highly irregular and discordant pluton margins commonly associated with host rock blocks and rafts entirely enclosed by solidified magma suggest that thermal cracking, stoping, and by inference assimilation also occur during pluton emplacement (e.g. Clarke et al., 1998). Such mechanisms could remove evidence of earlier high strain in the inner aureoles (Paterson and Vernon, 1995), resulting in an incomplete record of directly measurable ductile aureole strain. Later in this paper, we discuss some effects of stoping and/or assimilation on previously formed ductile aureole strain and the implications for preserving evidence for fast strain rates.

3. Numerical model

For direct comparison with the kinematic models of Johnson et al. (2001) and Gerbi et al. (2004), we use a spherical geometry and compare our results with a final pluton radius of 5 km (Fig. 2A). The kinematic models assume a constant volumetric fill rate through a feeder dike and do not evaluate the thermal evolution. Hence, the kinematic models are sensitive to fill rate only because they do not incorporate any mechanical host rock response. In this paper, we include stress- and temperature-dependent behavior of the aureole to explore thermo-mechanical coupling. Note that Fig. 2 can represent a central section of any orientation when used for comparison with the kinematic models. For comparison with natural examples, however, Fig. 2 is best viewed as a horizontal section because most field exposures of pluton aureoles are approximately horizontal surfaces and, given the small pluton radius compared with the thickness of the crust, vertical gradients are not considered in this study.

Despite the recent popularity of magma transport via feeder dikes (e.g. Clemens and Mawer, 1992; Petford et al., 1993; McNulty et al., 1996) we note that this is only one end member among other means of magma supply, including pervasive flow (Weinberg, 1999) decompression melting associated with nested diapirism (Weinberg, 1997), and complex combinations of the above are also possible. However, the exact nature and interplay of these processes are essentially unknown and consequently any attempt to implement these in a numerical model would necessarily rest much on speculation. Therefore, we make the simplifying assumption that magma is supplied into the chamber by any viable means and that constant pressure is maintained in the chamber. The main use of this end-member

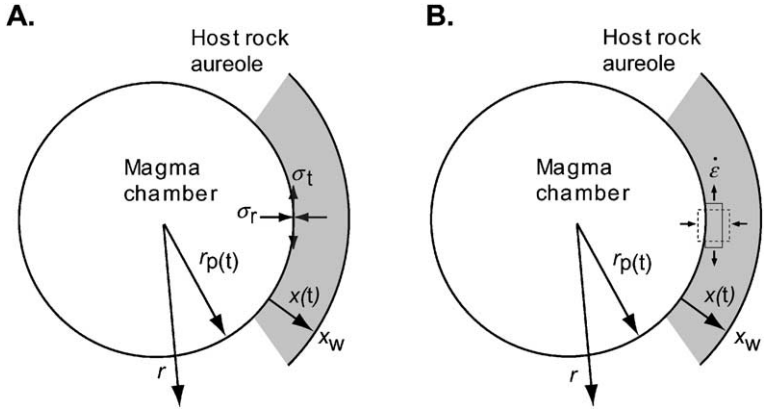

Fig. 2. Model geometry. (A) r is distance from pluton center. Pluton radius r_p and aureole width x increase as a function of time. σ_r and σ_t depict radial and tangential stress, respectively. (B) Maximum stretching direction represents direction of maximum strain rates $\dot{\varepsilon}$.

model is to maintain a driving force for pluton growth, to obtain first-order estimates of strain rate variation, and examine how they feed back into the growth behavior. Later in this paper, we discuss some of the most obvious implications concerning variable magma pressure.

We acknowledge the potential importance of preexisting fabrics, strain hardening and multiphase rocks in the crust, but because our goal is to study first-order rheological effects during emplacement these aspects are not considered in the present paper. In keeping with our simple approach, we consider the aureole to be composed of wet quartzite. A polymineralic aureole would be more realistic, but quartz is the most thoroughly studied crustal mineral (e.g. Hirth and Tullis, 1992) and it is common throughout the middle and upper crust. Examples of quartz-rich aureoles (McNulty et al., 1996; Yoshinobu and Girty, 1999) and interconnected weak layers of quartz in some aureoles (e.g. Albertz, 1999) suggest that a mono-mineralic approximation of the model aureole is applicable in at least some instances. The trade-off of our approach is that wet quartz yields faster strain rates at the conditions tested than polymineralic aggregates, but the advantage is that we can avoid the difficulty associated with the dependence of polyphase aggregate strength on strengths, volume proportions, and geometric arrangements of their components, all of which can change with progressive strain (e.g. Dell'Angelo and Tullis, 1996).

The ductile aureole is defined as the zone of dislocation creep, bounded by the magma-host rock interface on one side, and the outer aureole edge, x_w, on the other side (Fig. 2A). x_w is set where the temperature exceeds 300 °C in the host rock, a value at which dislocation creep in quartz-bearing rocks typically dominates (Hirth and Tullis, 1994; Stöckhert et al., 1999, and references therein).

We apply a dislocation creep flow law of the form:

$$\dot{\varepsilon}(x) = Af^m\sigma^n e^{\frac{-Q}{RT}} \quad (1)$$

where $\dot{\varepsilon}$ is the strain rate at position x within the aureole, A is the pre-exponential constant, f is the water fugacity, m is the fugacity exponent, σ is the differential stress, n is the stress exponent, Q is the activation energy, R is the universal gas constant, and T is the temperature. Parameters for this flow law were experimentally determined by Luan and Paterson (1992) and Gleason and Tullis (1995). Subsequent work by Hirth et al. (2001) tested the flow law against natural constraints and produced the physical parameters that we use (Table 1).

Similar to rock deformation experiments, we assume that a given rock volume undergoing deformation in our model aureole is shortening parallel to the direction of maximum principal stress and extending in the direction(s) of minimum principal stress (Fig. 2A). The associated length change as a function of time represents the strain rate (Fig. 2B). Several field (e.g. Paterson and Fowler, 1993; Paterson et al., 1996) and theoretical (e.g. Weinberg and Podladchikov, 1994) studies indicate that the power law behavior of ductile aureoles requires them to be quite narrow. Thus, the lateral far-field MTPs are likely to be elastic and inconsequential in terms of permanent records of ductile strains (and order-of-magnitude changes in strain rate) considered in this study. Consequently, the aureole can be thought of as a series of shells that become thinner as the pluton grows, and the displaced material is brought towards Earth's surface and/or returned to the magma generation site via far-field MTPs.

Although we are primarily interested in the temporal and spatial variation of strain rates through the aureole, it is a useful exercise to determine the expected maximum rates of homogeneous dislocation creep. Applying Eq. (1), the magma pressure used in this study (100 MPa) and a temperature close to the melting point of crustal rocks (650 °C) results in a maximum possible strain rate on the order of $10^{-10}\,s^{-1}$. We demonstrate below the circumstances under which these strain rates occur at the pluton margin and evaluate whether they are likely to be preserved. Because stress and temperature vary with time and position in the aureole, we require a coupled thermo-mechanical

Table 1
Modeling parameters

Parameter		Value	Unit
Activation energy	Q	135	kJ mol^{-1}
Pre-exponent constant	A	6.3×10^{-12}	MPa^{-n} s^{-2}
Water fugacity	f	37	MPa
Fugacity exponent	m	1	
Stress exponent	n	4	
Universal gas constant	R	8.3144	J mol^{-1} K^{-1}
Chamber-internal pressure	P	100	MPa
Specific heat	C (magma, aureole, host rock)	1000	J kg^{-1} K^{-1}
Density	ρ Magma	2550	kg m^{-3}
	ρ Aureole	2650	kg m^{-3}
	ρ Host rock	2750	kg m^{-3}
Coefficient of heat conduction	κ (magma, aureole, host rock)	1	W m^{-1}K^{-1}
Ambient host rock temperature	T_{host}	300	°C
Magma emplacement temperature	T_{magma}	850	°C

Parameters A, f, m and n from Hirth et al. (2001). Magma emplacement temperature = liquidus from Wyllie (1971) and Scaillet et al. (1995).

solution. We define the differential stress at any given time that enters the flow law as the maximum shear stress (Eq. 2-60 in Turcotte and Schubert, 2002):

$$\sigma(x) = \frac{1}{2}(\sigma_r - \sigma_t) \tag{2}$$

where σ_r and σ_t are the radial and tangential stress components (Fig. 2B), respectively, given by:

$$\sigma_r = P\frac{r_p^3}{(r_p + x)^3} \tag{3}$$

and

$$\sigma_t = -P\frac{r_p^3}{2(r_p + x)^3} \tag{4}$$

where P is the magma pressure in the chamber, r_p is the pluton radius, and x is position within the aureole. Because, to date, direct measurements of magma pressures in natural plutons are not possible, we utilize indirect constraints to define the magma pressure in our study. Utilizing the relationships for magma pressure first stated in Baer and Reches (1991), Hogan et al. (1998) determined that at depths shallower than the brittle–ductile transition magma pressure can range from ca. 60 to 150 MPa. Field and microstructural observations in other geologic settings (e.g. mylonites in the Eastern Alps, Italy (Stöckhert et al., 1999); Ruby Gap duplex, Australia (Hirth et al., 2001)) show that differential stresses of 60–160 MPa are consistent with dislocation creep in quartz. On this basis, we chose a value of $P = 100$ MPa, which is within the range of differential stresses recorded by dislocation creep microstructures in the rocks studied by Stöckhert et al. (1999) and Hirth et al. (2001), and smaller than the expected lithostatic pressures (used as a proxy for brittle yield stress) in our study.

Magma pressure in real plutons may vary considerably through time, for example in chambers characterized by batch arrivals of magma. We can qualitatively predict that short time intervals between magma batches would have a relatively small effect on the integrated results, and correspondingly, that long time intervals would have larger effects. However, the nature of such variation is speculative, and we choose a constant magma pressure which, in effect, allows us to examine an end-member emplacement model in which the time frame of magma arrival is relatively fast, whether or not it comes in a single batch or many smaller ones. The boundary condition of temporally constant magma pressure yields maximum strain rates at any given time and position in the model aureole. In Section 5, we explore the circumstances under which dislocation creep strain rates are particularly sensitive to pressure changes.

We apply an explicit implementation of the one-dimensional finite difference method (Croft and Lilley, 1997) to solve the one-dimensional heat conduction equation (Ranalli, 1987)

$$C_\rho \frac{\partial T}{\partial t} = \kappa \frac{\partial^2 T}{\partial r^2} \tag{5}$$

where C is specific heat, ρ is density, T is temperature, t is time, κ is coefficient of heat conduction, and r is distance from the pluton center. Reduction to one dimension is permissible due to the radial symmetry of the model (the material properties do not vary with position). For a geothermal gradient of ca. 30 °C km^{-1} in arcs, an ambient far-field temperature of 300 °C represents a crustal depth of ca. 10 km.

In order to couple strain with aureole shortening in our modeling, at each node point the strain rate $\dot{\varepsilon}$ is converted to incremental strain ε using

$$\varepsilon = \dot{\varepsilon}\Delta t \tag{6}$$

where Δt is the time step increment. The incremental strains are then numerically integrated over the aureole width, x_w, to obtain the bulk aureole strain for a given time step:

$$\mathrm{d}r_p = \int_0^{x_w} \varepsilon(x)\mathrm{d}x \tag{7}$$

The bulk aureole strain directly feeds back into pluton growth because the aureole shortening corresponds to radial pluton growth. We reset the node parameters to account for growth and the time loop begins anew.

Because we are primarily interested in strain rates associated with pluton growth, the rates considered in the numerical model result from inflation of the model pluton only, and regional deformation is not considered. Strictly, the best locations in which to test emplacement-related strain rates obtained in this study (and in general) are those in which emplacement post-dates most or all of the regional ductile deformation (e.g. Johnson et al., 1999, 2004; Vernon et al., 2004). However, in a slightly more restricted sense our results can also be applied to syntectonic plutonism. For instance, regional shortening at typical rates of ca. 10^{-14} s^{-1} would have the strongest effect on emplacement-related rates of the same order of magnitude (i.e. 10^{-14} s^{-1}) by increasing the value of the strain rate by a factor of 2 (maximum estimate for parallel pluton inflation and regional shortening vectors), but would not yield order-of-magnitude changes.

4. Results

We investigate the effect of coupled stress and temperature on strain rates using three different models. Model 1: the liquidus temperature (850 °C, Wyllie, 1971; Scaillet et al., 1995) is maintained in the pluton center only, and deformation takes place by dislocation creep only in the host rock. Model 2: the liquidus temperature is maintained in the pluton center only, but the portions of the pluton that

have cooled below 650 °C (solidus from Wyllie, 1971; Scaillet et al., 1995) become part of the deforming aureole. Model 3: the liquidus temperature is maintained in the entire pluton, and deformation takes place by dislocation creep only in the host rock. Model times varied according to how long it took the chambers to grow to a final radius of 5 km. Hence, the simulations were calculated for 1.2 million years (model 1), 150,000 years (model 2) and 60,000 years (model 3) over a total radial distance of 15 km at 10 m node spacing. Figs. 3–5 show the results for stresses, temperatures, and strain rates. Table 2 lists the total pluton growth times, average fill rates, normalized thermal aureole widths, normalized structural aureole widths, and maximum strain rates for the three models. We summarize the results for plutons with finite radii of 5 km.

4.1. Model 1: Liquidus temperature maintained in pluton center, and dislocation creep occurs in host rock aureole

With time both the pluton radius, as well as the aureole width, increase (Fig. 3). The pluton grows to its final size of 5 km in ca. 1 million years. We illustrate changes in differential stress (Fig. 3A), temperature (Fig. 3B), and dislocation creep strain rates (Fig. 3C) as functions of time and aureole width. The stress and temperature values are highest close to the magma chamber margin and fall off over short distances. For example, during the early stages of chamber growth (ca. 10,000 years), temperatures of over 800 °C at the contact decrease to ambient host rock temperatures of 300 °C over a distance of only 1 km. The thermal aureole becomes considerably wider with time. At ca. half the chamber construction time (500,000 years), the thermal aureole is ca. 6.5 km wide. During most of the duration of magma chamber construction large portions of the aureole are at moderate temperatures of ca. 350–450 °C and the immediate contact between pluton and host rock is at ca. 500 °C.

Variations in strain rates follow a similar pattern. The highest host rock strain rates are on the order of $10^{-11}\,s^{-1}$ and occur very close to the pluton margin where stress and temperature are also at their maximum. The rates reduce to values on the order of $10^{-14}\,s^{-1}$, which is considered typical of regional deformation, at ca. 1–1.5 km distance from the pluton margin for much of the time before they become geologically insignificant ($\leq 10^{-15}\,s^{-1}$).

4.2. Model 2: Liquidus temperature maintained in pluton center, and dislocation creep occurs in outer portion of pluton and host rock aureole

In this section, we consider the deformation aureole to include those portions of the pluton that have cooled below 650 °C, and the host rock domain between the pluton margin and the outer edge of the aureole. This composite aureole contains both pluton and host rock, and undergoes deformation by dislocation creep.

The most striking difference to model 1 is the much shorter total pluton growth time of ca. 132,000 years for a finite radius of 5 km (Fig. 4A). We set the magma pressure in this model only for the region of the pluton that is ≥850 °C; therefore, the effective radius used to calculate the stress distribution in the composite aureole (Eqs. 2–4) remains short compared with model 1. Correspondingly, the

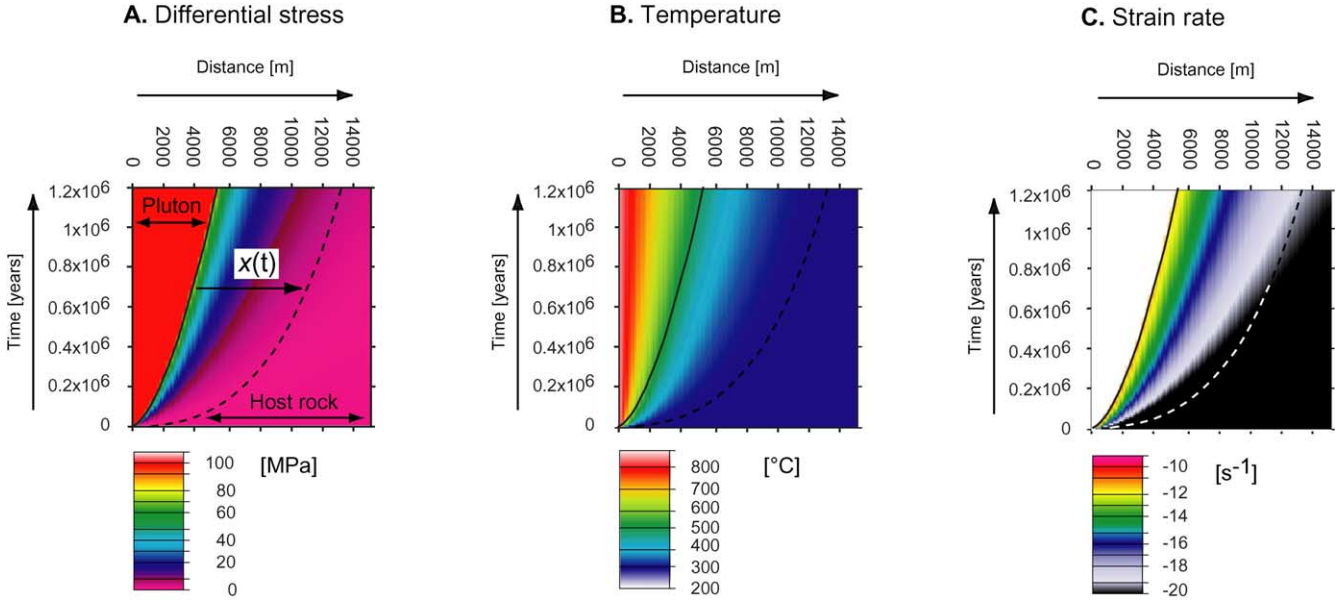

Fig. 3. Results of dislocation creep modeling for model 1. Horizontal axis shows distance from the center of the magma chamber. Vertical axis indicates modeling time. Solid black lines depict the interface between magma chamber and host rock. Dashed lines represent outer aureole edge, $x_w \geq 300$ °C. The following panels show the results computed along the aureole width, x as a function of time. (A) Differential stress. (B) Temperature. (C) Dislocation creep strain rate. $x(t)$ depicts width of host rock aureole.

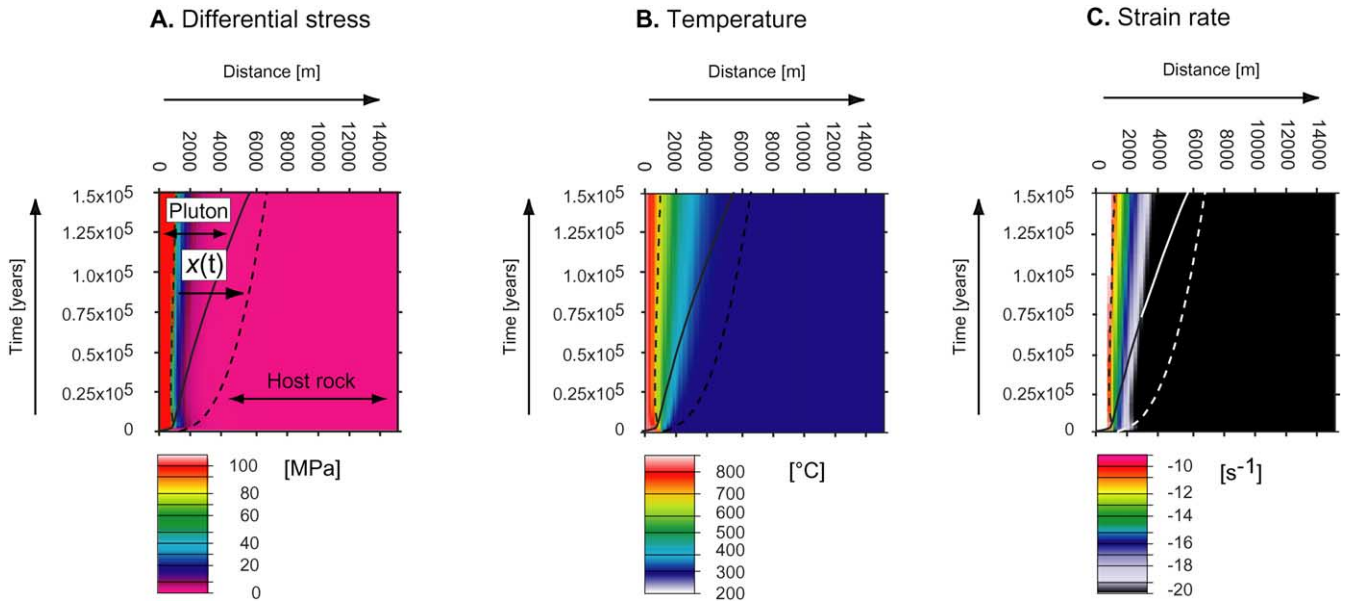

Fig. 4. Results of dislocation creep modeling for model 2. Panels as in Fig. 3. Solid black line tracks the position of the pluton margin through time. Dashed line in pluton indicates position of inner edge of bulk aureole. Dashed line in host rock as in model 1 (Fig. 3). $x(t)$ depicts width of bulk aureole (i.e. both pluton and host rock aureoles).

aureole width over which differential stress is applied also remains short (Fig. 4A).

Similar to model 1, the composite thermal aureole becomes wider with time, but it is ca. 2.2 km shorter than the thermal (host rock) aureole in model 1 (Figs. 3B and 4B). We observe another major difference with regard to the thermal behavior. Initially, the host rock thermal aureole is wider than the pluton thermal aureole, but after ca. 80,000 years these relationships switch; the pluton thermal aureole continues to become wider, whereas the host rock thermal aureole begins to progressively thin. Note also that after ca. 100,000 years, the pluton-related temperature gradient lies entirely in the pluton (Fig. 4B).

The strain rate distribution is somewhat similar to that in model 1. Maximum strain rates are confined to a narrow zone which now occurs at the interface between the liquid and solid portions of the pluton. Strain rates range from maximum values of ca. $10^{-10}\,s^{-1}$ to regional strain rates and less within ca. 1 km (Fig. 4C). Similar to the thermal characteristics, gradients in strain rate initially occur in the

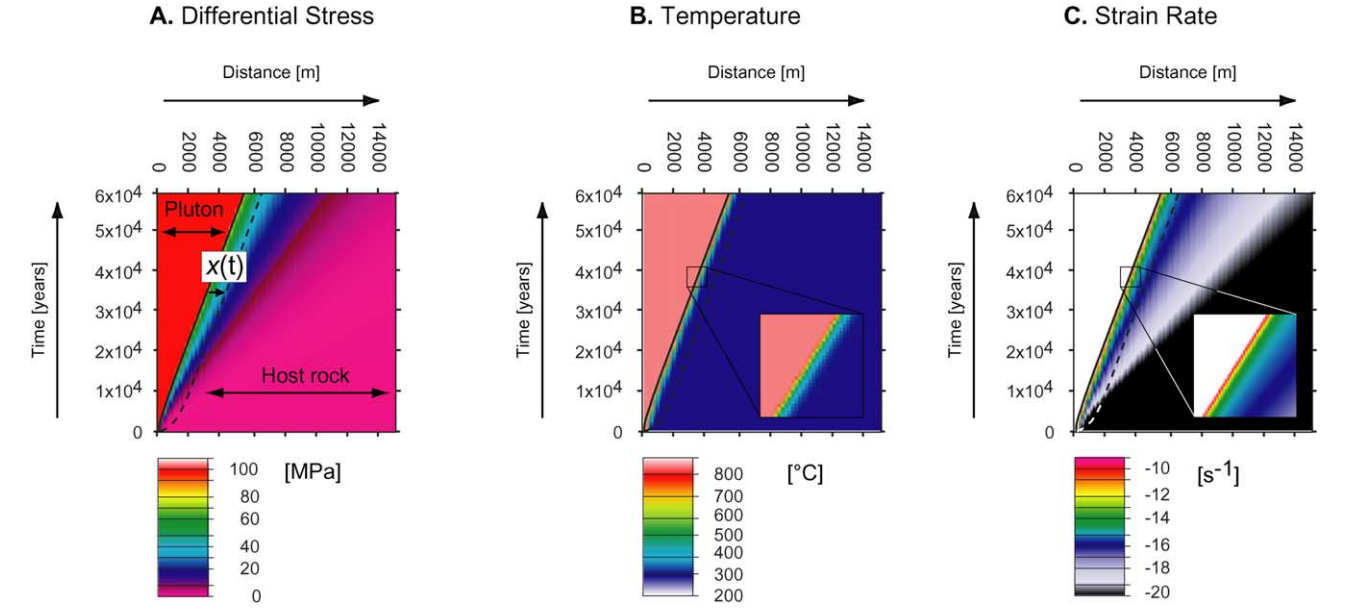

Fig. 5. Results of dislocation creep modeling for model 3. Panels as in Fig. 3. Insets show magnified portions of the aureole to show steep gradients in temperature and strain rate. $x(t)$ depicts width of host rock aureole.

Table 2
Modeling results for plutons with final radii of 5 km

Model	1	2	3
Total pluton growth time (10^5 years)	10.66	1.32	0.55
Average fill rate ($m^3\ s^{-1}$)	0.016	0.126	0.302
Normalized thermal aureole width	1.566	1.128	0.242
Normalized structural aureole width	0.360	0.180	0.067
Maximum strain rate (s^{-1})	10^{-11}	10^{-10}	10^{-10}
Maximum strain rate preserved after material removal (s^{-1})	10^{-14}	10^{-12}	10^{-16}

Normalized thermal aureole width = thermal aureole width/pluton radius. Normalized structural aureole width = structural aureole width (outer edge corresponds to a strain rate of $10^{-14}\ s^{-1}$)/pluton radius.

host rock structural aureole but they completely shift into the pluton with time. For example, after ca. 25,000 years, the portions deforming at rates faster than $10^{-14}\ s^{-1}$ occur only in the pluton. The fundamental difference between this and the other models considered (see below also) is that, once the pluton has grown to a final radius of 5 km, any gradients in stress, temperature, and strain rate are entirely located in the pluton.

4.3. Model 3: Liquidus temperature maintained in entire pluton, and dislocation creep occurs in host rock aureole

To explore the strongest possible effect of temperature and stress on strain rates and thus further bracket natural systems, we consider an extreme end member in which the liquidus temperature is maintained in the pluton center throughout the model time. Among the three models we compare, model 3 shows the shortest pluton growth time of ca. 55,000 years (Fig. 5A). The stress distribution in the host rock aureole resembles the one indicated by model 1 (Figs. 3A and 5A). The similarity is due to the fact that in models 1 and 3 we set the magma pressure for the entire pluton, whereas in model 2 this is done only in the liquid pluton center.

The most striking characteristic of model 3 is the extremely narrow width of the thermal aureole. The finite aureole width is only ca. 1.2 km and, except for the first few time steps, the thermal aureole width stays constant (Fig. 5B). The strain rate distribution is generally similar to that of the previous two models. The highest strain rates on the order of ca. $10^{-10}\ s^{-1}$ occur only immediately at the interface between the liquid pluton and the deformation

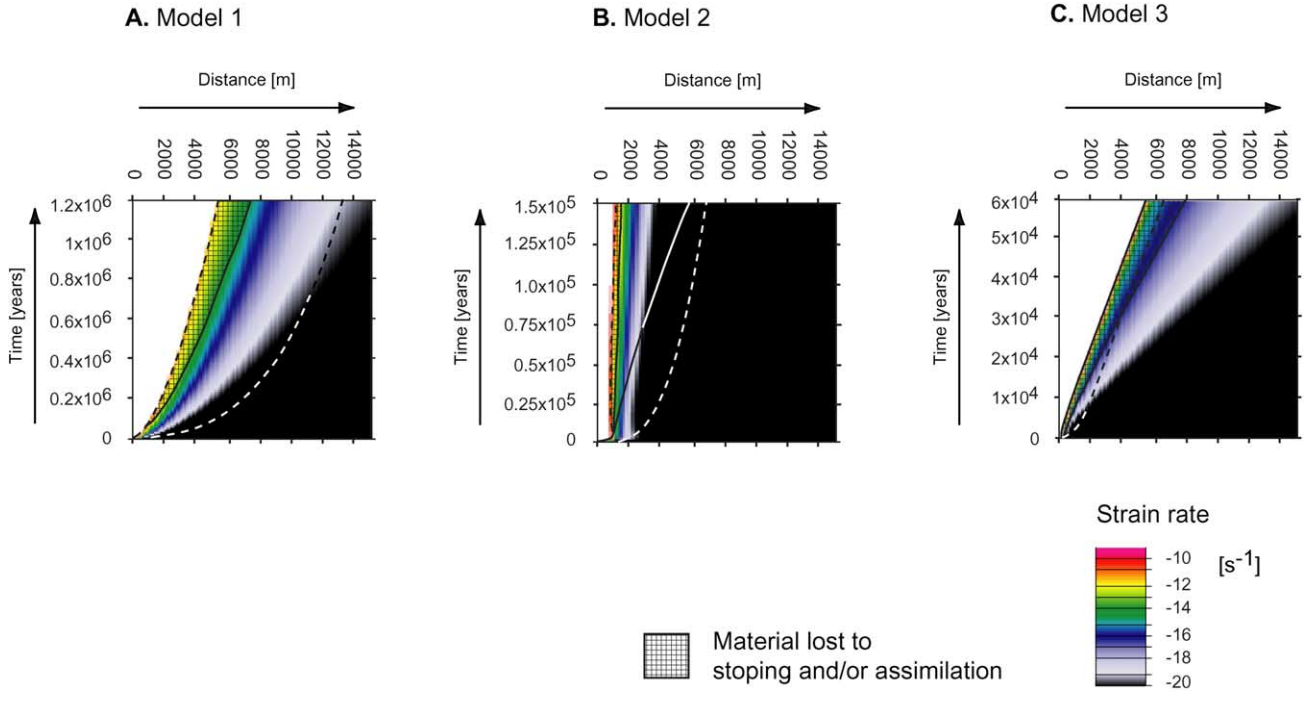

Fig. 6. Effect of material removal by stoping and/or assimilation on the preservation of strain rates in aureoles. Shaded regions show material (and potential documentation for strain rates) lost to stoping and/or assimilation. Solid lines show the positions of the pluton margins after stoping material removal has occurred. (A) Model 1. (B) Model 2. (C) Model 3. Note that these panels should be read differently than the panels in Figs. 3–5. Each time step represents the growth history of an individual hypothetical pluton. For example (Fig. 6A), at 100,000 years, 40% of the final pluton size ($r_p = 1000$ m) has been accommodated by dislocation creep. The remaining 60% is provided by material removal (i.e. now r_p is ca. 1357 m and the corresponding aureole width is removed).

aureole (Fig. 5C). Likewise, the zones deforming at strain rates faster than regional deformation become wider with time. In fact, this characteristic is more pronounced than in models 1 and 2. For example, in models 1 and 2, the strain rate variation from maximum to regional rates occurs within ca. 1/6 and 1/4 of the aureole widths, whereas in model 3, the equivalent change occurs over ca. 1/2 of the aureole width.

4.4. Effect of material removal by stoping and/or assimilation

In view of the potential loss of inner aureoles (Buddington, 1959; Paterson and Vernon, 1995), it is instructive to consider aureoles in which previously formed ductile structures are removed, as opposed to being strained. Removal of aureole material is most likely accommodated by stoping and/or assimilation. For example, stoped blocks in the Beer Creek Pluton in the White Mountains, CA, show structural fabrics and features characteristic of the deformation aureole (Albertz et al., 2000). This observation suggests removal of emplacement-related, ductily deformed aureole rocks by stoping and presumably assimilation at some stage during emplacement. The exact timing between ductile aureole strain and stoping and/or assimilation is unknown, but it is theoretically possible that crustal plutons grow to a certain size by ductile MTPs alone before stoping and/or assimilation become important. Alternatively, stoping and/or assimilation may happen early, when adjacent wall rocks are relatively cool and the lateral growth rate of the chamber is at its peak.

To examine the strongest possible impact of stoping and/or assimilation on the preservation potential of ductile structures in aureoles, we consider a scenario in which a hypothetical pluton grows to 40% of its final size, with associated host-rock material transfer occurring by dislocation creep alone. The remaining 60% of the necessary space is accommodated by subsequent stoping and/or assimilation. In terms of material removal from our model aureoles we think that stoping and assimilation are equally permissive and probably related in nature. Hence, we do not distinguish between these two processes and refer to them as 'material removal' in the remainder of this paper. Fig. 6 should be read in the following way. Any time section (e.g. 100,000, 200,000 years, etc. in Fig. 6A) represents growth of up to 40% of a pluton's final volume. The remaining 60% volumetric growth is accommodated by material removal and hence loss of aureole rocks that previously underwent ductile deformation by dislocation creep. The shaded areas in Fig. 6 depict the additional amounts of radial growth of

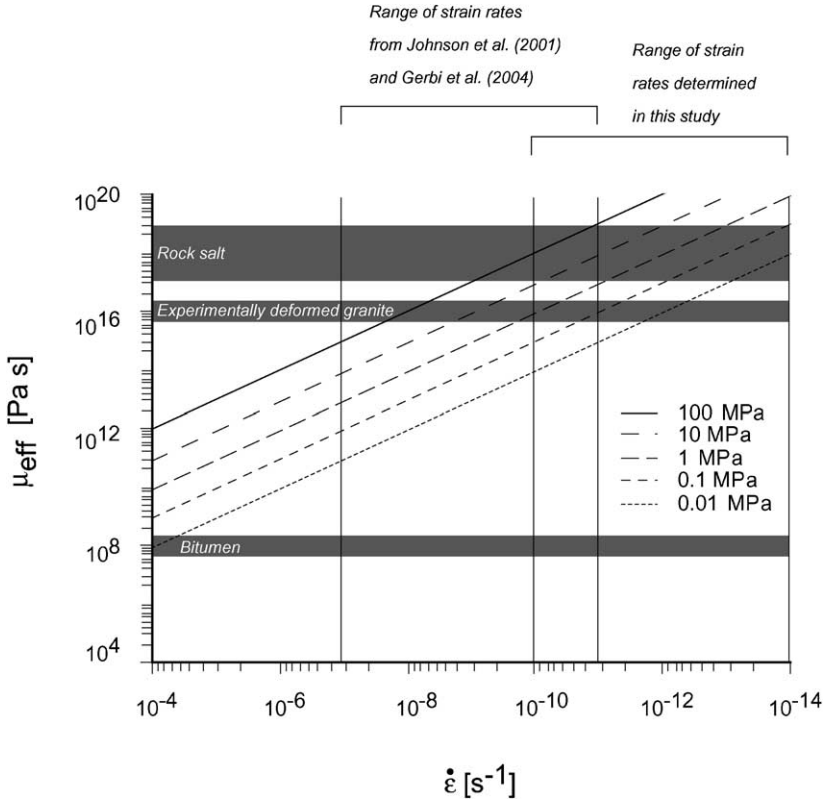

Fig. 7. Effective viscosity versus strain rate for differential stress values of 0.01–100 MPa. Horizontal lines indicate reference viscosities (from top to bottom) for rock salt (Jackson et al., 1990), the lowest published viscosity of crustal rocks (Talbot, 1999), and bitumen at room temperature (Barnes et al., 1989). Vertical lines show the range of strain rates derived from kinematic modeling (Johnson et al., 2001; Gerbi et al., 2004) and from this study. The following equation was applied to calculate effective viscosity: $\mu_{\text{eff}} = \sigma/\dot{\varepsilon}$ (Poirier, 1985).

the plutons and thus the corresponding removal of the inner aureoles. The solid black lines show the position of the pluton margins after material removal has occurred. Fig. 6 suggests that in the end-member scenario considered, only model 2 can potentially preserve evidence for fast strain rates. Note, however, that, based on our understanding that stoping occurs at the juxtaposition of magma and solid rock, we used the effectively liquid pluton radius to estimate the additional space accommodation by material removal. As a result, the entire domain in which material removal occurs, lies within the pluton aureole. On the other hand, models 1 and 3 suggest that high-strain-rate inner aureoles can potentially be completely lost to subsequent material removal.

5. Discussion

5.1. Comparison with kinematic models

Our results show that rates of dislocation creep (10^{-10}–10^{-11} s^{-1}) higher than published rates of regional deformation (10^{-13}–10^{-15} s^{-1}) can occur only in a very narrow zone close to the pluton margin. These rates overlap with the slowest strain rates predicted in the kinematic models of dike-fed expansion (ca. 10^{-11} s^{-1}, Johnson et al., 2001; Gerbi et al., 2004). The kinematic models predict wall rock strain rates that span up to 6 orders of magnitude, owing to the cubed relation between radial and volumetric growth. The strain rates range from extremely high values of ca. 10^{-4} s^{-1} near the pluton margins and early in the expansion history, to values of ca. 10^{-13} s^{-1} farther away from the margins and later during the pluton growth. In contrast, our coupled thermo-mechanical modeling indicates that dislocation creep is limited to maximum rates of ca. 10^{-10} s^{-1} in narrow near-margin portions of some aureoles, decreasing to regional strain rates within short distances to the pluton margins. Consequently, the different strain rates obtained from the two modeling approaches entail different growth durations of spherically expanding plutons. For instance, the kinematic models of Johnson et al. (2001) predict pluton growth times of only ca. 0.13 and 1846 years for the fastest and slowest dike flow rates, respectively, whereas our model plutons require ca. 1 million years (model 1), 132,000 years (model 2), and 55,000 years (model 3) to grow to their final radius of 5 km.

The kinematic models predict wall rock strain rates between 10^{-7} and 10^{-11} s^{-1} for much of the emplacement history, depending on the assumed volumetric rate of magma transfer from the feeder dike to the growing chamber. To illustrate these magnitudes of strain rates in terms of crustal rheology, it is illustrative to convert them to effective viscosities (Fig. 7). For example, rocks undergoing ductile deformation at a strain rate of 10^{-7} s^{-1} and differential stresses of 10–100 MPa require the corresponding effective viscosities to be as low as 10^{14}–10^{15} Pa s. Note that this is 1–2 orders of magnitude lower than the lowest experimentally determined viscosity of crystalline granite (10^{16} Pa s; Talbot, 1999; Fig. 7) and that most of the effective viscosities required by the kinematic models are not confirmed experimentally. On the other hand, the maximum strain rates of 10^{-10}–10^{-11} s^{-1} determined in this study require effective viscosities of 10^{17}–10^{18} Pa s, which are fully in the range of the viscosities of rock salt (10^{17}–10^{19} Pa s; Jackson et al., 1990; Fig. 7).

Regarding the effect of material removal on the preservation potential of evidence for emplacement-related fast strain rates, our results are similar to those of Gerbi et al. (2004). We have shown above that in the extreme case where material removal occurs only after 40% of the space needed for the pluton has been accommodated by dislocation creep, the high-strain-rate inner aureole can potentially be completely removed. Likewise, Gerbi et al. (2004) illustrated that with higher degrees of stoping (i.e. 0, 20, and 50% of the total pluton volume) the aureole rocks immediately adjacent to the pluton margin are progressively less strained, resulting in overall less strained aureoles and lower normalized aureole widths.

In any case, if spherical plutons expand to their final size as rapidly as implied by the kinematic models, the possibility of brittle space accommodation and/or faster-than dislocation creep ductile deformation mechanisms should be considered. On the other hand, our study indicates that considerably slower expanding spherical plutons can displace their surrounding aureole rocks by dislocation creep alone. We elaborate on the effect of strain rates on the system evolution, the role of temperature and magma pressure, and then discuss the implications for pluton emplacement.

5.2. Effect of strain rates on system evolution

The three models we present in this study illustrate how the range and spatial distribution of strain rates in pluton aureoles may influence the growth behavior and also the physical nature of aureoles. For example, models 1 and 3 represent two extreme end members that are useful in discussing the effect of allowing the pluton to participate in cooling or keeping the entire pluton at the liquidus. Because in both cases, the stress distribution across the aureole is very similar, we can isolate the control of temperature on the strain rate distribution. Figs. 3B and 5B show that the maximum temperatures at the pluton margins in models 1 and 3 are ca. 500 and 650 °C, respectively. The corresponding strain rates at the contact are on the order of ca. 10^{-11} and 10^{-10} s^{-1}, respectively. Although the maximum rates differ only by one order of magnitude, the consequences are remarkable. The pluton growth time in model 3 is only ca. 1/20 of that in model 1. On the other hand, this dramatic difference should not be unexpected, given that an order-of-magnitude change in strain rate is equivalent to 10 times as much material displacement at a given point in an aureole.

Despite the obvious difference in pluton growth time between models 1 and 3, the higher maximum strain rates in

model 3 directly influence the finite width of the thermal aureole. Compared with model 1, the thermal aureole in model 3 is extremely thin and remains at constant width throughout the growth duration (Fig. 3B). This also is plausible, given that heat conduction is time-dependent and, considering the faster rates in model 3, there is simply less time available for a given aureole portion to conduct heat. In other words, model 1 represents a case in which the aureole deforms sufficiently slowly to allow for widespread heating (note that the isotherms are fanning). In contrast, model 3 represents the opposite end member; the radial pluton growth outpaces heat conduction (note that the isotherms are parallel and equidistant).

Model 2 represents a possible case between models 1 and 3. Analogous to model 1, the liquidus temperature is maintained only in the pluton center, but in this case the portions of the pluton cooled below the solidus participate in the deformation. The effect is that the composite deformation aureole is wider than in model 3 but narrower than in model 1 (Figs. 3–5). Maximum strain rates are locally also on the order of $10^{-10}\,s^{-1}$ but because for each time step, the surface area over which fast strain rates occur is smaller, the system cannot grow as rapidly as in model 3. However, the fast strain rates allow model 2 to grow considerably faster than model 1. With regard to preserving evidence for fast strain rates in aureoles, incorporating deformation in the

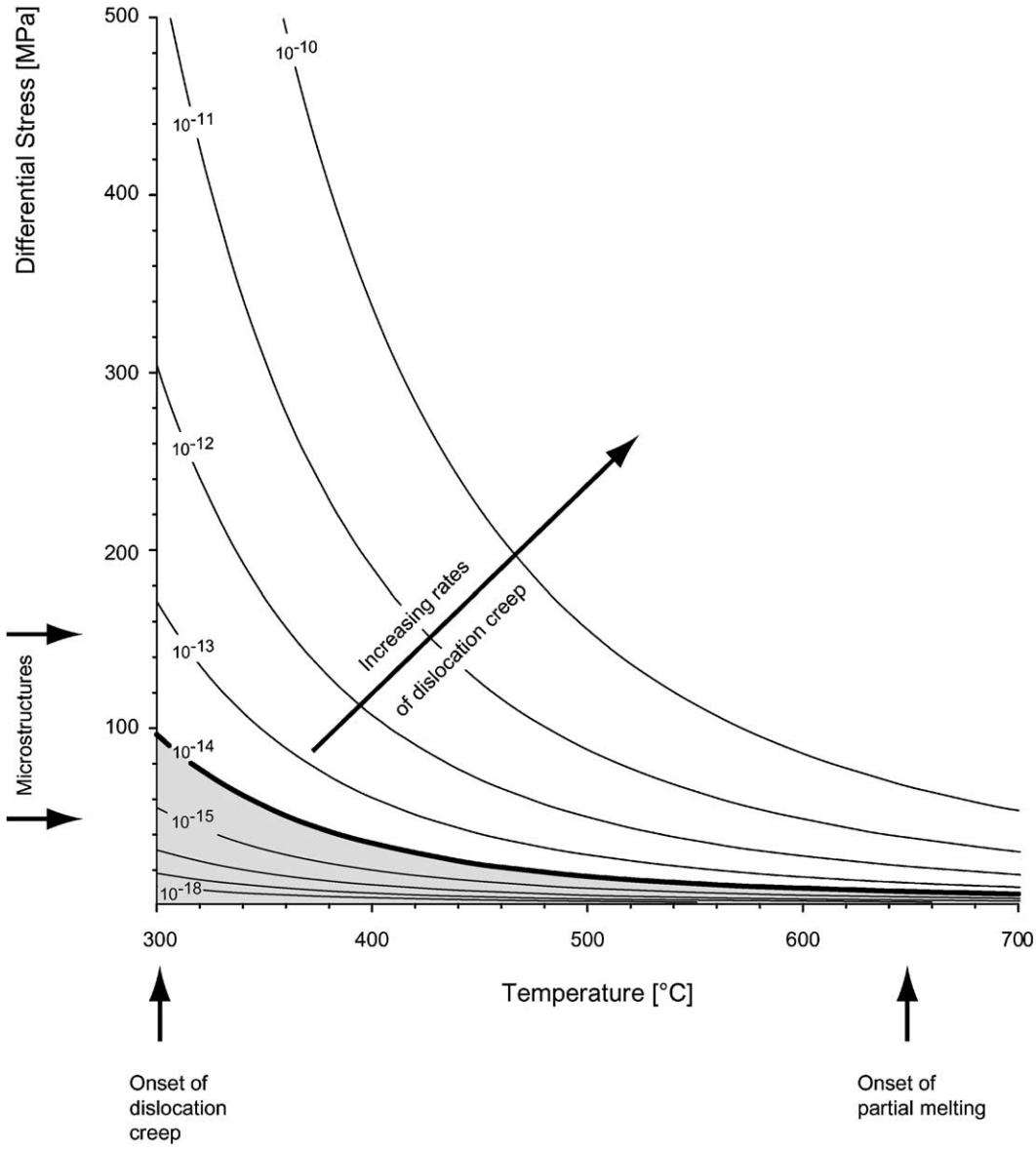

Fig. 8. Contour plot of dislocation creep strain rates as a function of differential stress and temperature using Eq. (1) and parameters of Hirth et al. (2001). Vertical arrows indicate temperatures at which the onsets of dislocation creep and partial melting occur. Horizontal arrows indicate range of differential stresses consistent with microstructures diagnostic of dislocation creep in natural settings. Shaded region depicts strain rates below typical regional strain rates of $10^{-14}\,s^{-1}$ and are geologically insignificant for the purpose of this study.

solidified pluton has first-order consequences. In the absence of material removal, models 1 and 3 imply the preservation of fast emplacement-related strain rates at the pluton margin (Figs. 3C and 5C). In contrast, the deformation exceeding rates of ca. 10^{-14} s^{-1} in model 2 takes place within the pluton and hence any evidence for fast strain rates would be completely absent in the host rock aureoles of such plutons (Fig. 4C).

5.3. Role of temperature and magma pressure

Although our knowledge about absolute values of magma pressure and periodic changes therein is extremely limited, it is instructive to discuss first-order effects of variable magma pressure on aureole strain rates. In order to explore the relationships between pressure, temperature, and resulting rates of dislocation creep, we plot strain rate contour lines (Fig. 8) using Eq. (1) of this study and parameters from Hirth et al. (2001). Fig. 8 shows strain rates spanning several orders of magnitude (10^{-18}–10^{-10} s^{-1}) for temperatures varying from 300 (the onset of dislocation creep) up to 700 °C (just above the onset of host rock melting) and pressures between 0 and 500 MPa.

First, we consider the outer edge of a hypothetical aureole where temperatures are at ca. 300 °C. Fig. 8 shows that the minimum pressure required for dislocation creep to occur at a regional strain rate (10^{-14} s^{-1}) is ca. 100 MPa. Furthermore, the diagram shows that an increase in strain rate by one order of magnitude (i.e. from 10^{-14} to 10^{-13} s^{-1}) requires an increase in magma pressure of ca. 70 MPa. On the other hand, the required temperature change for magma pressures between 50 and 150 MPa (this pressure range is consistent with microstructures indicative of dislocation creep; Stöckhert et al., 1999; Hirth et al., 2001) is ca. 60 °C or less. Hence, the switch from regional strain rates to faster-than-regional rates in the outer portions of the hypothetical aureole is sensitive to temperature as well as magma pressure.

Second, we consider the inner edge of a hypothetical aureole subjected to temperatures close to the onset of partial melting, for example ca. 600 °C. Fig. 8 indicates a dramatic difference in the sensitivity of strain rates to magma pressure. In this temperature domain, which is equivalent to near-margin rocks in some natural aureoles, strain rates are essentially sensitive only to magma pressure. Even a relatively small pressure increase of ca. 10 MPa raises the strain rate by one order of magnitude. Likewise, a ca. 30 MPa pressure increase raises the strain rate by two orders of magnitude without any required change in temperature.

Third, we consider the inner and outer portions of the aureole modeled in this study. The strain rate dependency on pressure and temperature in the outer edge of the model aureole is equivalent to the behavior of the outer edge of the hypothetical aureole discussed above. Despite lower temperatures in the inner edge of our model aureole compared with the hypothetical inner aureole, the behavior is also quite similar. For example, our thermal modeling predicts that, except for the first ca. 50,000 years (where temperatures are near the melting point of quartz-bearing rocks) most of the inner aureoles remain between ca. 500 and 650 °C for most the magma chamber growth (Figs. 3B, 4B and 5B). Fig. 8 shows that in the temperature domain of ca. 500–650 °C, any change in strain rates essentially depends on pressure changes only. For instance, an order of magnitude increase in strain rate (i.e. from 10^{-14} to 10^{-13} s^{-1}) requires a pressure increase of $\leq$20 MPa but no increase in temperature, and with progressively higher strain rates, increasingly larger pressure changes are required. Our results have several important implications for pluton emplacement, which we discuss below.

5.4. Implications for pluton emplacement

Fig. 8 illustrates that dislocation creep strain rates in aureoles that are subject to temperatures near the onset of partial melting are highly sensitive to pressure changes. It follows that dislocation creep strain rates in 'hot' inner aureoles may be subject to significant temporal variation in response to variation in chamber pressure. Several generations of magmatic dikes in many natural aureoles suggest that magma pressures drop and build up again frequently. Fig. 8 also demonstrates that strain rate drops require smaller pressure changes than strain rate jumps. Therefore, assigning single numerical values of strain rates for pluton margins deforming by dislocation creep has little relevance unless the corresponding values of magma pressure are known. We, therefore, suggest caution when determining strain rates associated with pluton emplacement; the inner parts of aureoles are highly dynamic, and strain rates may be subject to large variation.

Johnson et al. (2001) and Gerbi et al. (2004) proposed that evidence for fast strain rates in aureoles may be diagnostic of emplacement by dike-fed ballooning. Our dislocation creep modeling demonstrates that strain rates as fast as 4 orders of magnitude higher than typical regional deformation can occur at the pluton margin. However, in order to obtain a strain rate of 10^{-7} s^{-1} requires, even for the inner 'hot' portions of aureoles, unrealistically high magma pressures. Using Eq. (1) and a temperature range of 300–600 °C yields pressures of ca. 1–9 GPa independent of any particular emplacement model.

We and others have now begun to recognize potentially extremely fast deformation mechanisms in natural aureoles, including cataclastic flow in the San José pluton, Mexico (Johnson et al., 2003, 2004), melt-assisted granular flow in aureoles of the Tuolumne Intrusive Suite, California as well as the Mount Stuart Batholith, Washington (Albertz et al., 2005) and diffusion-accommodated grain boundary sliding in the Bergell pluton (Rosenberg and Stünitz, 2003). However, emplacement by nested diapirs or a combination of nested dike-fed pulses and nested diapirs cannot be ruled out in many cases. Therefore, evidence for fast strain rates

in pluton aureoles and strain rates in general may not be reliable criteria to differentiate among pluton emplacement mechanisms.

Another question is what range of strain rates should we expect to be preserved in an aureole in which the inner, highly strained portions have been removed? This question cannot be answered directly because the preservation of evidence for fast ductile strain rates in aureoles depends on the relative timing between material removal and ductile flow. To date we have no quantitative constraints on the temporal relationships between material removal and ductile flow. In the extreme case where material removal accommodates 60–70% of the space occupied by the pluton after the development of a ductile aureole, the complete body of field evidence for faster-than-regional strain rates can potentially be removed. If material removal and ductile flow by dislocation creep alternate in natural aureoles, after each removal event re-establishing steeper temperature gradients between magma and host rocks will allow higher rates of ductile flow in previously 'slowly' deformed portions of the aureole. Hence, we might expect the superposition of high strain rate structures on low strain rate structures. To quantify the temporal relationships between material removal and ductile flow, additional groundwork on the thermo-mechanical controls of material removal and integration with field studies is necessary.

Lastly, some aspects of our modeling have implications for preserving finite strains in structural aureoles around plutons. For example, field observations suggest that only ca. 30–40% of the material displacement necessary for magma emplacement can typically be accounted for in host rock aureoles (Paterson and Fowler, 1993; Paterson and Vernon, 1995). However, in view of the potentially complete shift of the deformation front into the pluton itself (Fig. 4), insufficient finite strains in host rock aureoles may in fact be expected. Fig. 4C indicates that during the second half of the growth duration, the host rock aureole is essentially completely static and all deformation takes place in the portion of the pluton that has cooled below its solidus. Although this is an end-member model, natural plutons may partition the deformation between the pluton and host rock aureoles in a different manner, potentially so that 30–40% ductile deformation takes place in the host rock aureole, and the remaining space is provided by deformation in the pluton and/or by material removal.

5.5. Comparison with natural examples

Natural pluton-host rock systems are more complex than the geometrically and mechanically simple theoretical end members described in this study. Despite the inherent limitations of our models, however, each of them yields useful and thought-provoking predictions that can be utilized to help interpret natural systems. For example, although it may be unrealistic to assume that the entire volume of a given mid-crustal magma chamber stays above the liquidus (our model 3), such an end member illustrates the thermomechanical behavior of a system whose aureole stays 'hot' for extended time periods. Thus, in the case of a natural pluton with magmatic fabrics extending to the pluton margin and an anomalously thin ductile aureole, the possibility certainly exists that the magma chamber grew so rapidly, that, regardless of pluton geometry, heat conduction lagged behind volumetric growth (in this case the possibility could also be entertained that chamber growth occurred by virtue of short-lived pulses, e.g. Albertz et al., 2005). On the other hand, a pluton exposing solid state fabrics in its outer portions and a somewhat wider aureole may be interpreted in terms of a composite aureole in which both solidified plutonic and host rock accommodated ductile shortening, indicating that in this case heat conduction kept pace with volumetric growth. With this in mind, we can compare several aspects of our model results with natural examples.

In terms of maximum strain rates during emplacement-related deformation, our results fit well with estimated strain rates from field-related studies (Karlstrom et al., 1993; John and Blundy, 1993; Miller and Paterson, 1994; Nyman et al., 1995; McCaffrey et al., 1999; Fernandez and Castro, 1999; Johnson et al., 2004). For example, Nyman et al. (1995) utilized 90% ductile thinning of the aureole rocks and thermal modeling to estimate aureole strain rates on the order of 10^{-12} s^{-1}, indicating that dislocation creep rates of 10^{-11} s^{-1} focused in a narrow zone of an aureole may have occurred but was not preserved in some natural systems. Using the effective pluton margins and a typical regional strain rate of 10^{-14} s^{-1} as boundaries, we can calculate the normalized structural aureole widths (Table 2). Our values range from 0.360 (model 1) over 0.180 (model 2) to 0.067 (model 3) and are within the range of normalized structural aureole widths obtained from natural plutons (0.05–0.66; Paterson and Fowler, 1993). Highly concentrated ductile strain was also found by previous theoretical studies that did not account for material removal (e.g. Weinberg and Podladchikov, 1994).

With regards to thermal implications, our results are in accordance with Johnson et al. (2004) who documented that the crystallized outer unit of the San José pluton in Baja California, México was intruded by an inner unit leading to solid-state fabric development at the outer margin. Our Fig. 4b indicates that during magma emplacement into the pluton center the outer portions of the magma chamber cool below typical solidus temperatures of granitoid rocks while the central portions remain magmatic. If the inner portions continue to grow, either continually or episodically, the outer, sub-solidus portions will begin to participate in solid-state deformation by dislocation creep and/or other processes.

6. Conclusions

We performed numerical modeling of dislocation creep as a ductile, near-field material transfer process during

radial pluton expansion using coupled spatial and temporal changes in stress and temperature. Given the principle assumptions of spherical pluton shape, initial and constant magma-chamber pressure of 100 MPa, magma emplacement temperature of 850 °C, negligible importance of far-field MTPs, and homogeneous aureole deformation by dislocation creep with and without subsequent material removal by stoping and/or assimilation, the present study yields the following major conclusions.

The computed stress and temperatures in the host rocks range from 100 to 10 MPa and 800 to 300 °C, respectively, resulting in rates of dislocation creep with maximum values of ca. 10^{-10} s^{-1} that are limited to a narrow zone close to the effective pluton margin. The strain rates become geologically insignificant over relatively short distances of 1–2 km. Large portions of the modeled aureole deform at regional strain rates of ca. 10^{-14} s^{-1} or only moderately faster. Maintaining a constant liquidus temperature in a pluton results in thin thermal and structural aureoles and short pluton growth times. The inner, 'hot' portions of the aureole are extremely sensitive to pressure changes, indicating that assigning single strain rate values to inner aureoles or extrapolating these over long time periods may be inadequate because dynamic pressure changes in natural plutons can lead to significant changes in host-rock strain rates.

The fast aureole strain rates calculated in this study indicate that strain rates in general may not be a reliable criterion to differentiate among pluton emplacement mechanisms. This is supported by evidence for extremely fast strain rates in aureoles of plutons that are consistent with emplacement models of both dike-fed pulses and nested diapirism. Regardless of which deformation mechanisms accommodate fast strain rates in natural aureoles the inner portions may be completely lost due to material removal. Hence, any evidence for strain rates may not be preserved in some aureoles.

Acknowledgements

Thorough and constructive reviews by Jan Tullis and Rick Law as well as helpful comments by Chris Gerbi enhanced an early version of this manuscript. This work was supported by NSF Grant number EAR-0440063, a German Academic Exchange Service (DAAD) grant and a Sigma Xi Grant-in-Aid of Research. We thank Scott R. Paterson and Charlie Sammis for scientific discussions, David Okaya for assistance with the numerical modeling, and two anonymous reviewers for their thoughtful comments.

References

Albertz, M., 1999. Structures in the western part and post-intrusive tilting of the Rieserferner Pluton, Eastern Alps (South-Tyrol, Italy), unpublished Diploma thesis, University of Giessen, 141pp.

Albertz, M., Wetmore, P.H., Pignotta, G.S., Potter, M.E., Andreasson, G., Paterson, S.R., 2000. How do magma chamber-host rock systems evolve through time? Abstracts with Programs—Geological Society of America 32, 1.

Albertz, M., Paterson, S.R., Okaya, D., 2005. Fast strain rates during pluton emplacement: magmatically folded leucocratic dikes in aureoles of the Mount Stuart Batholith, Washington and the Tuolumne Intrusive Suite, California. Geological Society of America Bulletin 117, 450–465.

Baer, G., Reches, Z., 1991. Mechanics of emplacement and tectonic implications of the Ramon dike System, Israel. Journal of Geophysical Research 96, 11,895–11,910.

Barnes, H.A., Hutton, J.F., Walters, K., 1989. An Introduction to Rheology, Rheology Series, Vol. 3. Elsevier, Amsterdam.

Bateman, P.C., 1992. Plutonism in the central part of the Sierra Nevada batholith, California. US Geological Survey Professional Paper 1483.

Buddington, A.F., 1959. Granite emplacement with special reference to North America. Geological Society of America Bulletin 70, 671–747.

Clarke, D.B., Henry, A.S., White, M.A., 1998. Exploding xenoliths and the absence of "elephants' graveyards" in granite batholiths. Journal of Structural Geology 20, 1325–1343.

Clemens, J.D., Mawer, C.K., 1992. Granitic magma transport by fracture propagation. Tectonophysics 204, 339–360.

Coleman, D.S., Glazner, A.F., 1997. The Sierra Crest magmatic event: rapid formation of juvenile crust during the Late Cretaceous in California. International Geology Review 39, 768–787.

Croft, D.R., Lilley, D.G., 1997. Heat Transfer Calculations Using Finite Difference Equations. Applied Science Publishers, England.

Dell'Angelo, L.N., Tullis, J., 1996. Textural and mechanical evolution with progressive strain in experimentally deformed aplite. Tectonophysics 256, 57–82.

Fernandez, C., Castro, A., 1999. Pluton accommodation at high strain rates in the upper continental crust: the example of the central Extremadura Batholith, Spain. Journal of Structural Geology 21, 1143–1150.

Gerbi, C., Johnson, S.E., Paterson, S.R., 2004. Implications of rapid, dike-fed pluton growth for host-rock strain rates and emplacement mechanisms. Journal of Structural Geology 26, 583–594.

Gleason, G.C., Tullis, J., 1995. A flow law for dislocation creep of quartz aggregates determined with the molten salt cell. Tectonophysics 247, 1–23.

Gudmundsson, A., 1990. Emplacement of dikes, sills, and crustal magma chambers at divergent plate boundaries. Tectonophysics 176, 257–275.

Hirth, G., Tullis, J., 1992. Dislocation creep regimes in quartz aggregates. Journal of Structural Geology 14, 145–159.

Hirth, G., Tullis, J., 1994. The brittle–plastic transition in experimentally deformed quartz aggregates. Journal of Geophysical Research 99, 11, 731–11,747.

Hirth, G., Teyssier, C., Dunlop, W.J., 2001. An evaluation of quartzite flow laws based on comparisons between experimentally and naturally deformed rocks. International Journal of Earth Sciences 90, 77–87.

Hogan, J.P., Price, J.D., Gilbert, M.C., 1998. Magma traps and driving pressure: consequences for pluton shape and emplacement in an extensional regime. Journal of Structural Geology 20, 1155–1168.

Jackson, M.P.A., Cornelius, C.M., Gansser, C.A., Seöcklin, J., Talbot, C.J., 1990. Salt diapirs of the Great Kavir, Central Iran. Memoirs of the Geological Society of America 177, 139.

John, B.E., Blundy, J.D., 1993. Emplacement-related deformation of granitoid magmas, southern Adamello massif, Italy. Geological Society of America Bulletin 105, 1517–1541.

Johnson, S.E., Paterson, S.R., Tate, M.C., 1999. Structure and emplacement history of a multiple-center, cone-sheet-bearing ring complex: the Zarza Intrusive Complex, Baja California, México. Geological Society of America Bulletin 111, 607–619.

Johnson, S.E., Albertz, M., Paterson, S.R., 2001. Growth rates of dike-fed plutons: are they compatible with observations in the middle and upper crust? Geology 29, 727–730.

Johnson, S.E., Fletcher, J.M., Fanning, C.M., Vernon, R.H., Paterson, S.R., Tate, M.C., 2003. Structure, emplacement and lateral expansion of the

San José tonalite pluton, Peninsular Ranges batholith, Baja California, Mexico. Journal of Structural Geology 25, 1933–1957.

Johnson, S.E., Vernon, R.H., Upton, P., 2004. Foliation development and progressive strain-rate partitioning in the crystallizing carapace of a tonalite pluton: microstructural evidence and numerical modeling. Journal of Structural Geology 26, 1845–1865.

Karlstrom, K.E., Miller, C.F., Kingsbury, J.A., Wooden, J.L., 1993. Pluton emplacement along an active ductile thrust zone. Geological Society of America Bulletin 105, 213–230.

Knipe, R.J., 1990. Microstructural analysis and tectonic evolution in thrust systems: examples from the Assynt region of the Moine Thrust Zone, Scotland. In: Barber, D.J., Meredith, P.G. (Eds.), Deformation Processes in Minerals, Ceramics and Rocks. Mineralogical Society of Great Britain and Ireland, pp. 228–261.

Luan, F.C., Paterson, M.S., 1992. Preparation and deformation of synthetic aggregates of quartz. Journal of Geophysical Research 97, 301–320.

McCaffrey, K.J.W., Miller, C.F., Karlstrom, K.E., Simpson, C., 1999. Synmagmatic deformation patterns in the Old Women Mountains, SE California. Journal of Structural Geology 21, 335–349.

McNulty, B.A., Tong, W., Tobisch, O.T., 1996. Assembly of a dike-fed magma chamber; the Jackass Lakes Pluton, central Sierra Nevada, California. Geological Society of America Bulletin 108, 926–940.

Miller, R.B., Paterson, S.R., 1994. The transition from magmatic to high temperature solid state deformation: implications from the Mount Stuart Batholith, Washington. Journal of Structural Geology 16, 853–865.

Nyman, M.W., Law, R.D., Morgan, S.S., 1995. Conditions of contact metamorphism, Papoose Flat Pluton, eastern California, USA: implications for cooling and strain histories. Journal of Metamorphic Geology 13, 627–643.

Paterson, S.R., Fowler Jr., T.K., 1993. Re-examining pluton emplacement processes. Journal of Structural Geology 15, 191–206.

Paterson, S.R., Vernon, R.H., 1995. Bursting the bubble of ballooning plutons: a return to nested diapirs emplaced by multiple processes. Geological Society of America Bulletin 107, 1356–1380.

Paterson, S.R., Fowler Jr., T.K., Miller, R.B., 1996. Pluton emplacement in arcs: a crustal-scale exchange process. Geological Society of America Special Paper 315, 115–123.

Petford, N., Kerr, R.C., Lister, J.R., 1993. Dike transport of granitoid magmas. Geology 21, 845–848.

Pfiffner, O.A., Ramsay, J.G., 1982. Constraints on geological strain rates: arguments from finite strain states of naturally deformed rocks. Journal of Geophysical Research 87, 311–321.

Poirier, J.-P., 1985. Creep of Crystals. High-Temperature Deformation Processes in Metals, Ceramics and Minerals, Cambridge Earth Science Series. Cambridge University Press, Cambridge.

Price, N.J., 1975. Rates of deformation. Journal of the Geological Society of London 131, 553–575.

Ranalli, G., 1987. Rheology of the Earth: Deformation and Flow Processes in Geophysics and Geodynamics. Allen & Unwin, Boston, MA.

Rosenberg, C.L., Stünitz, H., 2003. Deformation and recrystallization of plagioclase along a temperature gradient: an example from the Bergell tonalite. Journal of Structural Geology 25, 389–408.

Scaillet, B., Pichavant, M., Roux, J., 1995. Experimental crystallization of leucogranite magmas. Journal of Petrology 36, 663–705.

Stöckhert, B., Brix, M.R., Kleinschrodt, R., Hurford, A.J., Wirth, R., 1999. Thermochronometry and microstructures of quartz—a comparison with experimental flow laws and predictions on the temperature of the brittle–plastic transition. Journal of Structural Geology 21, 351–369.

Talbot, C.J., 1999. Can field data constrain rock viscosities? Journal of Structural Geology 21, 949–957.

Turcotte, D.L., Schubert, G., 2002. Geodynamics. Cambridge University Press, Cambridge, UK.

Vernon, R.H., Johnson, S.E., Melis, E.A., 2004. Emplacement-related microstructures in the margin of a deformed pluton: the San José tonalite, Baja California, México. Journal of Structural Geology 26, 1867–1884.

Weinberg, R.F., 1997. Diapir-driven crustal convection; decompression melting, renewal of the magma source and the origin of nested plutons. Tectonophysics 271, 217–229.

Weinberg, R.F., 1999. Mesoscale pervasive felsic magma migration: alternatives to dyking. Lithos 46, 393–410.

Weinberg, R.F., Podladchikov, Y., 1994. Diapiric ascent of magmas through power law crust and mantle. Journal of Geophysical Research 99, 9543–9559.

Wyllie, J., 1971. The Dynamic Earth: Textbook in Geosciences. Wiley, New York. 416pp.

Yoshinobu, A.S., Girty, G.H., 1999. Measuring host rock volume changes during magma emplacement. Journal of Structural Geology 21, 111–116.